Proc. Natl. Acad. Sci. USA
Vol. 73, No. 9, pp. 2991–2994, September 1976
Biochemistry

Three dimensional structure of erabutoxin b neurotoxic protein: Inhibitor of acetylcholine receptor

(snake venoms/x-ray analysis/postsynaptic membrane/neuromuscular transmission/invariant residues)

BARBARA W. LOW, HUGH S. PRESTON*, ATSUSHI SATO†, LAWRENCE S. ROSEN, JAMES E. SEARL‡, ANDREW D. RUDKO§, AND JANE S. RICHARDSON¶

Department of Biochemistry, Columbia University, College of Physicians and Surgeons, 630 West 168 Street, New York, N.Y. 10032

Communicated by Paul A. Marks, May 21, 1976

ABSTRACT **The three-dimensional structure of erabutoxin b, a neurotoxin in the venom of the sea snake *Laticauda semifasciata*, has been determined from a 2.75 Å resolution electron density map. Erabutoxin b is one of a family of snake venom neurotoxins, all low-molecular-weight proteins, which block neuromuscular transmission at the postsynaptic membrane. They specifically inhibit the acetylcholine receptor.**

The molecular shape is that of a shallow elongated saucer with a footed stand formed by the six-membered ring at the COOH-terminal end. The central core of the molecule is an assembly of four disulfide bridges. Three long chain loops emerge as broad fronds from the core region. Approximately 40% of the main chain is organized into a twisted antiparallel β-pleated sheet of five short strands. In 28 snake venom neurotoxins of established sequence which inhibit the acetylcholine receptor, the four disulfide bridges and seven other residues remain invariant. Three substitution positions conserve residue type. In one wing of the molecule, there is a broad shallow depression which may characterize the reactive site. It is populated by the seven invariant residues and two of the three type conserved residues. This region is "anchored" on the undersurface of the molecule by the hydroxyl group of Ser-9, the remaining conservatively substituted residue.

Erabutoxin b is a protein neurotoxin of low molecular weight from the venom of the sea snake *Laticauda semifasciata* which blocks neuromuscular transmission at the postsynaptic membrane (1), in a nondepolarizing curare-like mode. The toxin binds at the cholinergic receptor site (2). Neurotoxins from sea and land snakes in the families *Hydrophiidae* and *Elapidae* show close structural homology (3) and a common mode of action (4–7). These neurotoxins specifically inhibit the acetylcholine membrane receptor protein (8, 9).

Three neurotoxins of *Laticauda semifasciata* are basic (isoelectric point >pH 9.2) single-chain proteins with 62 amino-acid residues and four disulfide bridges (10–12). Erabutoxins a and c are both single-substituted variants of erabutoxin b. The sequences of seven sea snake toxins, all with 60–62 residues, show multiple sequence substitutions and a dipeptide deletion in two toxins (3). When both sea and land snake neurotoxins are considered, the common mode of action and structural homology of 28 toxins is conserved through a broader range of sequence changes which include substitutions and deletions as well as insertions and COOH-terminal extensions. There remain the four invariant disulfide bridges as well as seven other invariant residues and three substitution positions which conserve residue type (see Fig. 1). We use the erabutoxin b sequence enumeration throughout.

Preliminary x-ray diffraction studies (13, 14) of erabutoxin b and the toxic erabutoxin b iodinated at His-26 (15) were reported and some features of earlier electron density maps at 5 Å and 2.9 Å described (16). In the orthorhombic crystal, space group $P2_12_12_1$, employed in this study, $a = 50.01$ Å, $b = 46.69$ Å, and $c = 21.43$ Å; there is one molecule per asymmetric unit. The molecule is an elongated concave disk or shallow saucer with foot. Two long chain regions that consist of well-defined loops were recognized in the 2.9 Å electron density map (16). Other regions were not unambiguously interpretable.

We describe here the structure of erabutoxin b as determined by x-ray crystallographic analysis from a 2.75 Å electron density map. We discuss the dominant features of secondary structure and attempt to relate to structure and function the spatial distribution of those invariant amino-acid residues which appear to be implicated in neurotoxic activity: the inhibition of acetylcholine receptor. A detailed report of this study will be published elsewhere.

METHODS

Crystals grown at pH 6.4 (13) were used to prepare two heavy atom derivatives by immersion in buffered solutions of (*a*) 1.5 mM K_2PtBr_4 and (*b*) 0.5 mM K_2PtCl_4. The chemically modified erabutoxin b iodinated at His-26 crystallizes at this pH. Crystals grown at pH 9.5 were isomorphous with the pH 6.4 preparations and of higher quality. They were grown from Tris·HCl buffer after addition of Na_2SO_4·NaOH at pH 9.5. The mother liquor was 11 mM Tris·HCl and 0.65 M Na_2SO_4; it contained 44.4 mg/ml of erabutoxin b. The crystals were used to collect intensity data which were not significantly different from those of crystals grown at pH 6.4. The pH 9.5 crystals gave new derivatives after immersion in buffered solutions of 2.5 mM *p*-hydroxy-*m*-mercuribenzoate for 2 days, and 25 mM $HgCl_2$ for five and three days, respectively. (These crystals were washed after soaking in $HgCl_2$-free buffer.)

Most of the x-ray diffraction data were collected on a General Electric XRD-490 diffractometer using nickel-filtered CuK_α radiation. The set of native protein data at pH 9.5 and data for one derivative were collected on a Syntex $P2_1$. Three standard reflections were monitored every 25 measurements. These were used to correct for crystal deterioration. Reflections were corrected for background, Lorentz and polarization effects, and a semi-empirical absorption correction was applied (17). The scaling of native to derivative data uses the method suggested by Kraut *et al.* (18, 19). Wilson plots were also calculated and agreed well with the absolute scale established.

* Present address, Department of Science, Government of Australia, Canberra, A.C.T.
† Present address, Department of Chemistry, Tohoku University, Sendai, Japan.
‡ Present address, Goddard Institute for Space Studies, 2880 Broadway, New York, N.Y. 10025.
§ Present address, New York City Housing and Development Administration, 100 Gold Street, New York, N.Y. 10038.
¶ Visiting investigator, Permanent address: Department of Anatomy, Duke University, Durham, N.C.

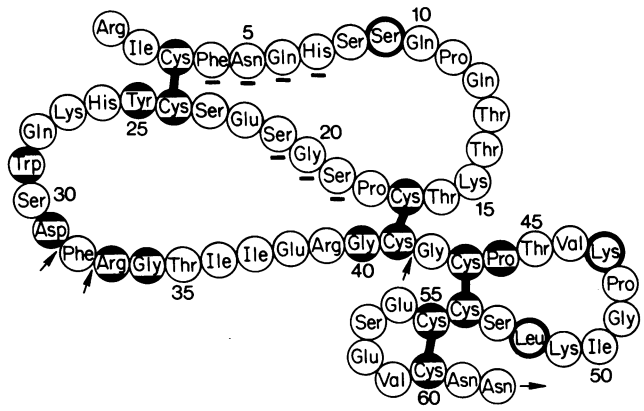

FIG. 1. Amino-acid sequence of erabutoxin b. The invariant residue positions in neurotoxins are shown emphasized by black caps, top and bottom. The three positions of conservative substitutions Ser-9, Lys-47, and Leu-52 are shown with a broader black outline. Horizontal lines under residues indicate observed deletion positions and arrows show observed insertion and COOH-terminal residue extension positions.

Heavy Atom Positions. These were first located in difference Patterson maps for the centric projections. Three-dimensional difference Patterson functions were sometimes also calculated. Heavy atom positions were related to a common origin by use of the Rossman function (20). The positions found were checked both by the calculation of difference Fourier syntheses using single isomorphous replacement phases from one derivative and multiple isomorphous replacement phases as the number of derivatives increased. Residual Fourier syntheses were used for preliminary refinement of all heavy atom positions. A three-dimensional iterative refinement procedure was used to refine the heavy atom positional parameters. For each iteration, all the native protein phases were determined from the current values of the parameters which were then refined by a least squares procedure to reduce the lack of closure of the phase angle triangles (21). The final overall figure of merit was 0.73 after six cycles of refinement.

The data on heavy atom derivatives were used to the limits shown in Table 1, to calculate the Fourier synthesis. These limits were chosen conservatively, after study of the distribution of the ratios of the root-mean-square lack of closure error to the mean heavy-atom scattering. The ratios were calculated as a function of $\sin\theta$ in shells.

Electron Density Map. The refined parameters were used to compute the final phase angles for the calculation of both best and most probable Fourier syntheses (22). The electron density map used for chain tracing was calculated in 36 sections perpendicular to c and drawn to a scale of 0.5 cm/Å. A map cut perpendicular to a was also used. Contours were drawn at intervals of 0.2 electrons/Å^3. The α carbon positions were marked on the map and a backbone model of the structure then built. Side chain group identification was based on the established sequence.

RESULTS

The molecular outline, recognized at lower resolution (16), is shown in the packing diagram (Fig. 2). Chain continuity is largely maintained at the level 0.6 electrons/Å^3 and some carbonyl protuberances can be seen. There are a few regions of close intermolecular approach. At only one of these, between Pro-18 and the Thr-35 of an adjacent molecule, was an arbitrary cut necessary. A few regions of apparently close intramolecular contact occur near the disulfide bridges, which form the central core of the molecule, even though only three are joined by half-cystines in near sequence relationship. The left-hand inset (Fig. 2) shows the main chain conformation and disulfide bridges. The three long chain loops, residues 2–17, 24–41, and 43–54, form the broad lobes of the molecular outline; a short turn defines the tapered neck region. Long loops are foreshortened in this projection (see Fig. 2 right-hand inset); they emerge as broad fronds from the central core region of disulfide bridges.

Table 1. Refinement statistics

Derivative*	N†	Z‡	R(Å)§	R_k¶	E‖
Hg3 (1)	3	20, 20, 9	4.3	0.11	24.9
Eb. I	3	21, 9, 6	3.8	0.18	45.8
Hg1	3	18, 12, 11	3.4	0.04	11.8
$PtCl_4^{2-}$	4	24, 14, 10, 3	3.2	0.10	25.2
$PtBr_4^{2-}$	5	55, 33, 32, 30, 15	2.75	0.15	36.9
Hg3 (2)	4	40, 33, 22, 10	2.75	0.12	29.9

* Abbreviations for heavy atom derivatives. Hg3, $HgCl_2$; Eb.I, erabutoxin b iodinated at His-26; Hgl, *p*-hydroxymercuribenzoate.
† N, the number of heavy atom sites.
‡ Z, Heavy atom occupancies in electrons.
§ R(Å), Limit of data used in final phasing calculation.
¶ $R_k = \sum_h ||F_{pH}| - |F_p + f_H||/\sum_h |F_{pH}|$ calculated for all reflections h and where F_{pH} is the structure factor of the derivative, F_p for the protein and f_H for the heavy atoms.
‖ E, root-mean-square lack of closure error.

The molecule fits into an ellipsoidal envelope approximately 38 Å × 28 Å × 15 Å. The end-on view, approximately down the

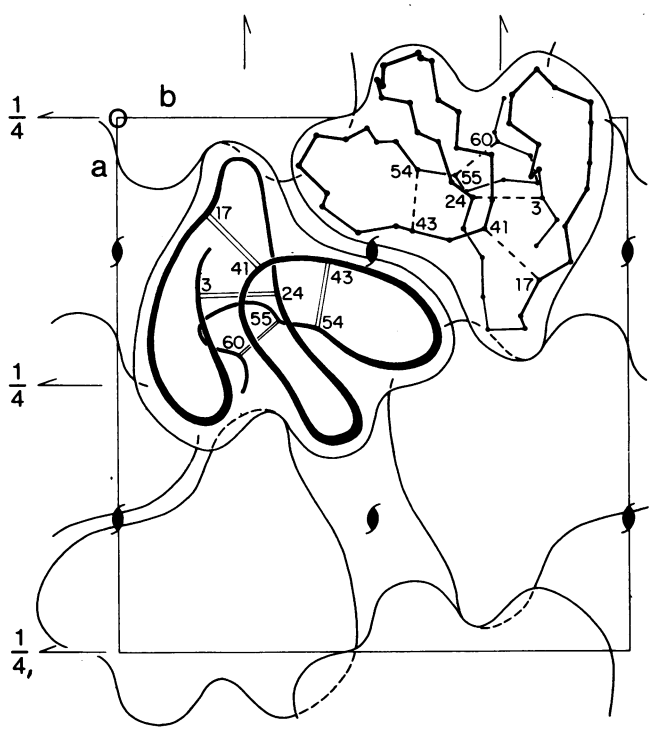

FIG. 2. Intermolecular packing diagram for erabutoxin b seen projected down the *c* axis. The left-hand inset drawing shows schematically the chain conformation and the disulfide bridge positions. The right-hand inset drawing shows the projected structure of a second erabutoxin b molecule related by a 2-fold screw axis parallel to *c*. Only α-carbon positions and disulfide bridges are shown.

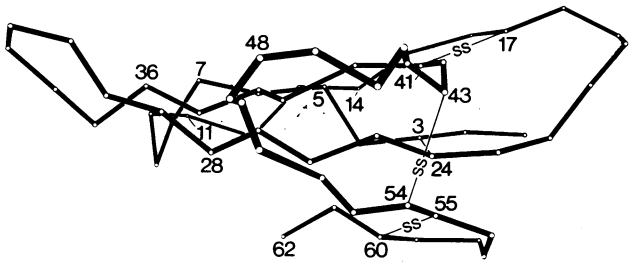

FIG. 3. The structure of erabutoxin b. Only α-carbon positions and disulfide bridges are shown. The residue positions enumerated are either half cystines or were chosen to indicate chain continuity.

b axis of the unit cell, (Fig. 3), shows the molecular shape: a shallow elongated saucer with footed stand formed by the six membered ring at the COOH-terminal end.

Conformation

Approximately 40% of the main chain is organized into a twisted antiparallel β-pleated sheet of five short strands. The positions of the strands in the sheet are βB, βA, βD, βC, βE (strands lettered in chain sequence order, see Fig. 4). The three central strands ADE are evident in the inset molecular drawings of Fig. 2. The loop which forms a crossover connection joining strands βD and βE is right handed (23). The disulfide core lies at one end of the β-sheet where the five β strands are joined. Minimum lengths of the β strands are B, 12–14; A, 4–8; D, 34–40; C, 25–31; and E, 51–53. There are at least 25 and possibly 31 residues in the sheet. There are β turns between strands B and A at residues 7–10, between strands D and C at residues 31–34, and between residues 47–50 and 18–21.

The presence of considerable regions of β structure in the neurotoxins was first proposed from studies of optical rotatory dispersion and circular dichroism (24). This accords with the conclusions of the laser Raman study (25) of erabutoxin b that extensive regions of antiparallel β-pleated sheet and of random coil coexist in the molecule. With Chou and Fasman's procedure (26), we predicted three β strand regions namely 2–6, 12–16 and 33–37 (observed 4–8, 12–14, 34–40), and two of the β turns 47–50 and 18–21. We have not made comparisons of the erabutoxin b structure and models proposed for the neurotoxins (27–29). Some correct predictions of β-turn region(s) were made by Gabel *et al.* (29) and Rydén *et al.* (27).

Residue distribution: Invariants and conservative substitutions

The presence of a central core of invariant disulfide bridges essential for toxicity (30) underscores a role of these linkages in maintaining functional groups in appropriate spatial relationships. All seven of the noncystine invariants and two of the three conservatively substituted residues lie within an oval outlined by the loop 32–48 . . . 32 in the left-hand wing of the molecule. Three of the invariant residues, Tyr-25, Gly-40, and Pro-44, are defined by Rydén *et al.* (27) as "structure" invariants because they, and the four disulfide bridges, are also invariant in related cardiotoxin and cytotoxin structures (3). Gly-40 is at a point of close approach of two chains, where a larger group would deform packing. Tyr-25 is not "buried" but is relatively inaccessible; it lies near Gly-40 and Pro-44.

The remaining four invariant residues Trp-29, Asp-31, Arg-33, and Gly-34 are neurotoxin "functional" invariants. Trp-29, the only tryptophan residue, is half-buried as was suggested by the fluorescence study (31). After modification of this residue, toxins lose activity (32, 33). The three remaining

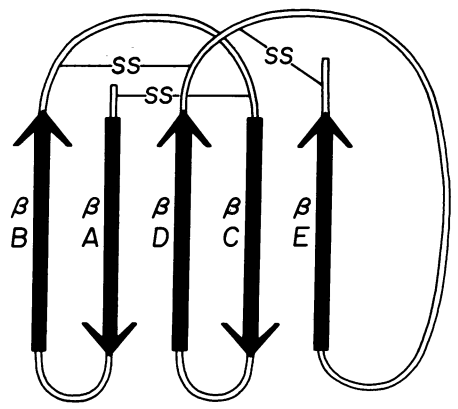

FIG. 4. Schematic representation of antiparallel β-pleated sheet structure in erabutoxin b. The strands are all joined by disulfide bridges as shown.

residues of this group 31, 33, and 34, are at one end (Fig. 3) of the longest loop. They define a β turn and, thus, are in relatively rigid conformation at the extreme left wing edge of the molecule. All three sites of conservatively substituted residues are restricted only in the neurotoxins; they are "functional" restrictions. Lys-47, an extended positively-charged side-chain group, which is substituted only by Arg, lies in the oval loop. Leu-52, the bulky conservative substituent points into the hole of the 43-54 ring. Only one conservatively substituted residue, the hydroxyl group Ser-9, is found outside on the lower molecular surface and it too is in the left-hand wing. There is, therefore, a broad shallow depression which may characterize the reactive site, populated by invariant residues and "anchored" at the left-hand corner underneath the depression by a hydroxyl group (Ser-9). The lower toxicity (approximately one-eighth that of the erabutoxins) of the atypical neurotoxin *Laticauda semifasciata* III is associated with loss of invariance at residue Asp-31, the hydroxyl in position nine, and the positive charge in position 47. The toxin has 66 residues; it is a neutral protein (34).

Structure-function relationships

If the reactive site of this inhibitor is indeed the broad shallow depression in the molecule where the invariant residues are found, then the reactive site of this inhibitor is similar to the active site of an enzyme. It is a cavity or depression into which, in this instance, the acetylcholine receptor may be expected to fit.

The assumption of topological molecular stability (that is the functional importance of the three-dimensional molecular structure we have found is attractive, particularly in view of the organization and distribution of invariant residues. But more studies must be undertaken, especially those of the inhibitor-acetylcholine receptor complex, before this hypothesis is validated.

We thank particularly Prof. Nobuo Tamiya, whose interests initiated and have stimulated this study, for his generous gifts of pure toxin and some of the crystals used. We thank Drs. David D. Dexter, Wardle W. Fullerton, and Jack Kay who made preliminary studies of heavy atom derivatives and worked (D.D.D.) in developing computer programs. One of us (B.W.L.) thanks the Japan Society for the Promotion of Science Visiting Professorship Program. This research was supported by Grants NS-07747 from the National Institutes of Health and BMS-73-01430 from the National Science Foundation and by the Columbia University Center for Computing Activities which made generous grants of computer time.

1. Tamiya, N. & Arai, H. (1966) *Biochem. J.* **99**, 624–630.
2. Sato, S., Abe, T. & Tamiya, N. (1970) *Toxicon* **8**, 313–314.
3. Tamiya, N. (1975) in *The Biology of Sea Snakes*, ed. Dunson, W. A. (University Park Press, Baltimore, Md.), pp. 385–415.
4. Chang, C. C. & Lee, C. Y. (1963) *Arch. Int. Pharmacodyn.* **144**, 241–257.
5. Raftery, M. A., Schmidt, J., Clark, D. G. & Wolcott, R. G. (1971) *Biochem. Biophys. Res. Commun.* **45**, 1622–1629.
6. Lee, C. Y. (1970) *Clin. Toxicol.* **3 (3)**, 457–472.
7. Hall, Z. W. (1972) *Annu. Rev. Biochem.* **41**, 925–952.
8. Miledi, R., Molinof, P. & Potter, L. T. (1971) *Nature* **229**, 554–557.
9. Changeux, J. P., Meunier, J. C. & Huchet, M. (1971) *Mol. Pharmacol.* **7**, 538–553.
10. Sato, S. & Tamiya, N. (1971) *Biochem. J.* **122**, 453–461.
11. Endo, Y., Sato, S., Ishii, S. & Tamiya, N. (1971) *Biochem. J.* **122**, 463–467.
12. Tamiya, N. & Abe, H. (1972) *Biochem. J.* **130**, 547–555.
13. Low, B. W., Potter, R., Jackson, R. B., Tamiya, N. & Sato, S. (1971) *J. Biol. Chem.* **246**, 4366–4368.
14. Preston, H. S., Kay, J., Sato, A., Low, B. W. & Tamiya, N. (1975) *Toxicon* **13**, 273–275.
15. Sato, S. & Tamiya, N. (1970) *J. Biochem. (Tokyo)* **68**, 867–872.
16. Low, B. W. (1975) "Symposium lecture, jubilee meeting Japanese Biochemical Society," *J. Biochem. (Tokyo)*, in press (abstr.).
17. North, A. C. T., Phillips, D. C. & Mathews, F. S. (1968) *Acta Crystallogr. Sect. A* **24**, 351–359.
18. Kraut, J., Sieker, L. C., High, D. F. & Freer, S. T. (1962) *Proc. Natl. Acad. Sci. USA* **48**, 1417–1424.
19. Arnone, A., Bier, C. J., Cotton, F. A., Day, V. W., Hazen, E. E., Jr., Richardson, D. C., Richardson, J. S. & Yonath, A. (1971) *J. Biol. Chem.* **7**, 2302–2316.
20. Rossman, M. G. (1960) *Acta Crystallogr.* **13**, 221–226.
21. Adams, M. J., Haas, D. J., Jeffery, B. A., McPherson, A., Jr., Mermall, H. L., Rossman, M. G., Schevitz, R. W. & Wonacott, A. J. (1969) *J. Mol. Biol.* **41**, 159–188.
22. Blow, D. M. & Crick, F. H. C. (1959) *Acta Crystallogr.* **12**, 794–802.
23. Richardson, J. S. (1976) *Proc. Natl. Acad. Sci. USA*, in press.
24. Yang, C. C., Chang, C. C., Hayashi, K., Suzuki, T., Ikeda, K. & Hamaguchi, K. (1968) *Biochim. Biophys. Acta* **168**, 373–376.
25. Harada, I., Takamatsu, T., Shimanouchi, T., Miyazawa, T. & Tamiya, N. (1976) *J. Phys. Chem.* **80**, 1153–1156.
26. Chou, P. & Fasman, G. D. (1974) *Biochemistry* **13**, 211–222.
27. Rydén, L., Gabel, D. & Eaker, D. (1973) *Int. J. Pept. Protein Res.* **5**, 261–273.
28. Smythies, J. R., Benington, F., Bradley, R. J., Bridgers, W. F., Morin, R. D. & Romine, W. O. (1975) *J. Theor. Biol.* **51(1)**, 111–126.
29. Gabel, D., Rasse, D. & Scheraga, H. A. (1976) *Int. J. Pept. Protein Res.*, **18**, 237–252.
30. Yang, C. C. (1967) *Biochim. Biophys. Acta* **133**, 346–355.
31. Chicheportiche, R., Rochat, C., Sampieri, F. & Lazdunski, M. (1972) *Biochemistry* **11**, 1681–1691.
32. Chang, C. C. & Hayashi, K. (1969) *Biochem. Biophys. Res. Commun.* **37**, 841–846.
33. Seto, A., Sato, S. & Tamiya, N. (1970) *Biochim. Biophys. Acta* **214**, 483–489.
34. Maeda, N. & Tamiya, N. (1974) *Biochem. J.* **141**, 389–400.